RESIDUAL STRENGTH ASSESSMENT AND DESTRUCTIVE TESTING OF DECOMMISSIONED CONCRETE BRIDGE BEAMS WITH CORRODED PRETENSIONED REINFORCEMENT

Rhys A. Rogers, BE, University of Auckland, Auckland, New Zealand
Liam Wotherspoon, PhD, University of Auckland, Auckland, New Zealand
Allan Scott, PhD, University of Canterbury, Christchurch, New Zealand
Jason M. Ingham, AP, University of Auckland, Auckland, New Zealand

ABSTRACT

Recent deterioration of pretensioned concrete bridge beams in New Zealand and Australia highlights an escalating problem. Pretensioned reinforcement corrosion is especially critical because of the highly stressed nature of the structures. Only a small amount of corrosion is required to a pretensioned strand before a considerable reduction of the structural capacity of the member occurs.

The Tiwai Point Bridge is located in a highly aggressive environment near Invercargill in the South Island of New Zealand. It consists of twenty seven 60 ft (18 m) spans; each span consists of nine 2‘3“ (686 mm) deep tee beams which contain both pretensioned and posttensioned reinforcement. The bridge was opened in 1969 and since that time chloride ingress has resulted in severe corrosion of the pretensioned reinforcement.

Each beam was subjected to a number of non-destructive corrosion assessment procedures. These results were used to estimate the ultimate strength of each beam. Each beam was then loaded to failure on a custom built four point flexural testing rig. The worst condition beams had damage to all four strands in the bottom layer and achieved strengths of 68% and 69% of their good condition counterparts.

The aim of this research was to assess the residual strength of beams which had experienced pretensioned reinforcement corrosion. The progression of corrosion damage observed in the beams was described and a model was presented for assessment of the beams using non-destructive means. The measured strength of the corroded beams was compared to nominally identical beams which had not experienced corrosion.

Keywords: Prestressed, Corrosion, Full Scale, Destructive, NDT,

TIWAI POINT BRIDGE

BACKGROUND

The Tiwai Point Bridge is located in a remote area near the very southern tip of the South Island of New Zealand. The bridge runs across Awarua Bay and provides the only road access to the New Zealand Aluminium Smelter, which is one of the largest industrial operations in NZ and accounts for a large proportion of the local region's economy[1]. The bridge was constructed specifically to serve the smelter and was opened in 1969. Awarua Bay provides a very harsh environment for a concrete structure due in particular to high winds prevailing across the structure, and the resultant salt spray which can penetrate concrete over time and cause the reinforcement to corrode.

While the bridge is on a public road, it leads only to the Aluminium Smelter and a small picnic area so the regular traffic volume is low and easily defined. A count in 2005 recorded 30 heavy vehicles per day[2] the majority of which were semi-articulated trucks carrying the maximum allowable load of smelted aluminium to the domestic market. Raw material and product bound for the international market was transported by sea directly from the wharf adjoining the smelter. Other regular traffic included 3 buses in and out of the plant twice a day carrying staff members and a small number of light vehicles carrying staff and contractors. Because there was no alternate land route the bridge was occasionally subjected to overloads, particularly during construction and maintenance operations at the smelter.

DESIGN AND CONSTRUCTION

The bridge was originally designed for the worst of two loading cases; the H20-S16-T16 design loading standard, or a single 100 T truck load restricted to travel over the central 5 beams. The H20-S16-T16 loading cases encompass traffic loads experienced during normal service of the bridge, while the 100 T overload case allowed for the delivery of plant required for construction and maintenance of the Aluminium Smelter.

The bridge consisted of twenty seven 18 m spans, each with nine 686 mm deep Tee beams transversely posttensioned together. The beams were precast and contained both pretensioned and posttensioned longitudinal reinforcement as well as transverse and shear reinforcement. The five central beams contained twelve 12.7 mm pretensioned strands each, while the two outside beams on each side contained ten pretensioned strands each. All beams contained one draped duct containing nine posttensioned 12.7 mm strands. Each posttensioned tendon ran for four spans between anchors, serving to provide some continuity between spans. Expansion joints were located between the anchors. The beams with an expansion joint at one end had a shallower parabolic drape to accommodate the anchor and different moment envelope.

The different pretension and posttension arrangements resulted in four beam types existing on the bridge, each with different longitudinal pretensioning configurations and thus considerably different ultimate limit state behaviour. In order from strongest to weakest, the

four beam types can be identified as: twelve pretensioned strands without an expansion joint, twelve pretensioned strands with an expansion joint, ten pretensioned strands without an expansion joint and ten pretensioned strands with an expansion joint.

A typical cross section of a beam is given in Fig. 1. An important feature of the design was that the shear reinforcement does not enclose the pretensioned strand. This detail causes the more critical pretensioned longitudinal reinforcement to corrode first and leads to a number of durability concerns[3].

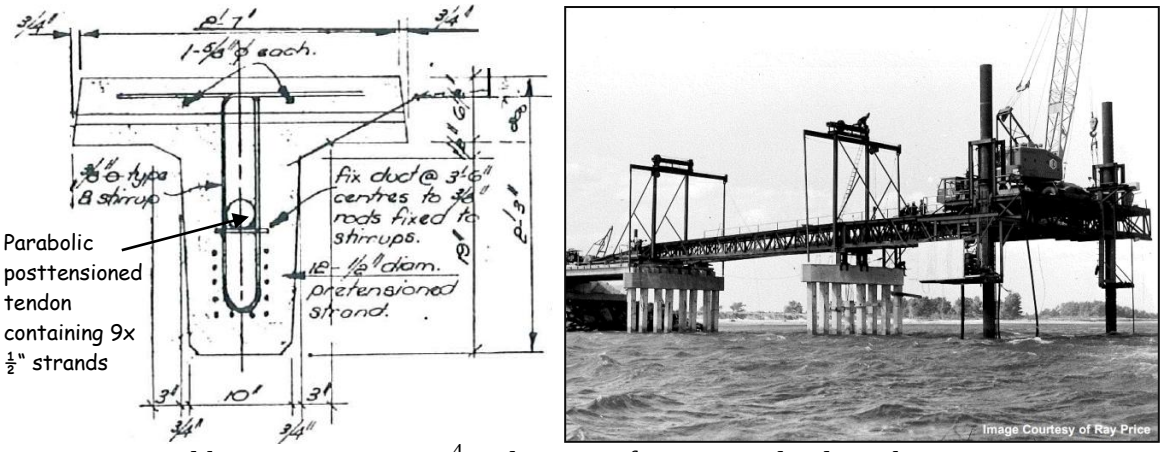

Fig. 1: Typical beam cross-section[4] and image of Tiwai Bridge launcher in operation

The bridge was constructed as part of the development of the Tiwai Point Aluminium Smelter which also included the construction of a dedicated wharf. The wharf structure consists of a pier head and a single lane access bridge. The superstructure of the access bridge is of similar design to the Tiwai Point Bridge. Both structures were constructed using the steel launcher and gantry system shown in operation in Fig. 1.

SERVICE LIFE AND INSPECTION HISTORY

During its service life the Tiwai Point Bridge was subjected to routine inspections on a 2 to 4 year cycle. These involved visual assessment of the bridge and fixtures from the roadway and abutments. As a result of these inspections several maintenance operations were carried out to the railings and other fixtures as they were identified. The regular inspection procedure allowed only for cursory inspection of the underside of the deck and beams as no means of access was allowed for.

In 2000 measurements of the depth to bed level at each pile set were taken to check for changes in the bed profile or scour around the piles. During this work extensive deterioration of the structure was noted and as a result a full inspection of the structure by boat was undertaken.

The reinforcement corrosion was a result of chloride ingress and was evidenced by longitudinal cracking along the sides of the beams at the level of the bottom layer of pretensioned strands. After a thorough investigation, it was estimated that in the worst cases this cracking correlated to a loss of up to 60% of the cross section of the bottom layer of pretensioned strands[1]. Several visual inspections were carried out to determine the prevalence of this damage, the most recent was in 2007 and found longitudinal cracking in fifty five of the two hundred and forty three beams[5].

Fig. 2 Corrosion induced cracking in side of web near soffit

Evidence of longitudinal cracking and rust staining in three beams from the same span is shown on the left of Fig. 2, and similar cracking in one beam is shown on the right. The maximum measured width for this type of crack was 5 mm and the cracking was consistently at the level of the bottom layer of pretensioned reinforcement.

After initial detection of the damage overloads were no longer permitted on the bridge and in 2004 weight and speed limits of 80% Class 1 loading and 30kph were applied to heavy traffic. After replacement was scheduled in 2006 the limits were relaxed to 100% Class 1 and 30kph, because consideration of the long term effects of overstressing the bridge was no longer required[2].

The original superstructure of the bridge was decommissioned and replaced in 2009 and 2010 due to widespread and severe corrosion of the pretensioned strand that was identified in the beams. The piers and pile caps were also in a deteriorated state, but these were rehabilitated and reused.

NON DESTRUCTIVE TESTING (NDT)

The aim of the Non Destructive Testing program was to identify and quantify the corrosion in the pretensioned strands within each concrete beam. This information was used to estimate the amount of effective pretensioned reinforcement for comparison with the destructive test results. This section gives an overview of the NDT techniques employed and a brief summary of the results.

VISUAL INSPECTION

A detailed visual inspection was undertaken and any identified defects were mapped and photographed. Details specific to each beam were recorded, such as the width of flanges, pull-in of cut posttensioning tendons and hog in beams.

Visual inspection results identified small patch repairs on some of the beams resulting from corrosion of stirrups or metal detritus accidentally cast into the concrete. This was concentrated in the haunches and in the soffit of the webs. Small areas of poor compaction were evident on many of the beams, but these did not reliably coincide with areas of visible corrosion damage. A high proportion of beams had some minor cracking and spalling evident on the sides of the haunches, consistent with corrosion of stirrups which had lower design cover in this region. In eight of the nineteen tested beams longitudinal cracks along the sides of the web were evident at the height of the pretensioned reinforcement. This cracking was often accompanied by rust staining and was caused by corrosion of the pretensioned reinforcement.

Following destructive testing of the beams a survey of the corrosion damage was taken in the area of broken concrete around the failure plane. The survey identified varying degrees of corrosion of the pretensioned strands, almost exclusively occurring to those strands in the bottom layer. The survey found no damage to the strands or duct making up the posttensioned tendon, and found the duct to be well grouted. In several cases some light surface corrosion was noted on the posttensioned strands; however, in these cases it was confirmed that there was no loss of cross section on any of the strands or wires in the tendon.

COVER DEPTH SURVEY

A cover survey was performed using an electromagnetic cover meter to determine the depth of cover to the pretensioned reinforcement and stirrups. The results indicated that the average cover to the pretensioned strand was 59 mm. The minimum measured cover to strand was 38 mm and the average of the minimum strand cover measured in a given beam was 50 mm. External evidence of strand corrosion did not correlate to a low cover depth.

Cover to stirrups was measured only in the haunches as these were the only areas where stirrups were shallower than pretensioned reinforcement. The average measured cover to stirrups was 39 mm, the lowest cover was 14 mm and the average of the minimums was 24.5 mm. Low cover depth correlated strongly to external evidence of stirrup corrosion.

ELECTRO POTENTIAL MAPPING (EPM)

EPM measures the difference in potential between the reinforcement embedded in the concrete and a reference electrode embedded in a hand held sensor. The measured potential is considerably more negative in areas where active corrosion of the reinforcement exists[6]. EPM was performed on the sides of the web and the soffit to identify sites of active corrosion

which were not visible on the surface of the concrete. While no strand corrosion was identified in areas without cracking, EPM assisted in the location of fine longitudinal cracks which had gone unnoticed in the visual inspection. The method is not able to determine the corrosion rate or the extent of damage.

EPM results have been analysed and the results show a strong relationship between very negative readings (red cells with a reading more negative than -350mV) and visual signs of corrosion such as longitudinal cracking in the sides of the web. High EPM readings correlated very closely with regions of strand failure. Fig. 3 gives an example of an EPM map of the web of a beam. The beam has been cut into four sections so that the entire length can be shown on the page. Each column represents five readings at one section of the beam, two readings from each side of the web and one from the soffit. Red cells indicate areas with a very high likelihood of corrosion, yellow and orange indicate some likelihood and green cells indicate low likelihood. In this case there is a very active area of corrosion just south of the centre line, and some likelihood of corrosion at the south end of the beam. In the destructive test beam 2C displayed a flexural failure in the red EPM region, and breakout of the concrete after the test confirmed that all four of the bottom pretensioned strands were severely corroded and unable to carry load.

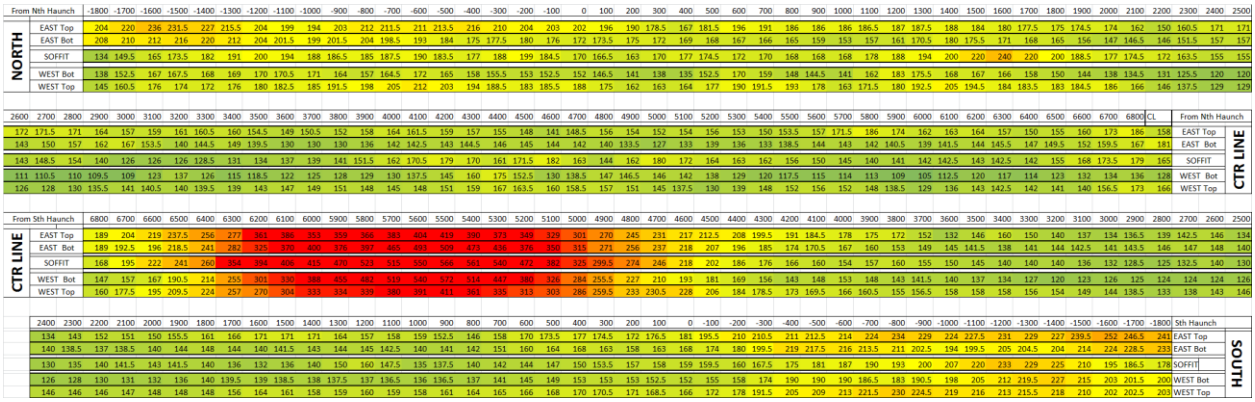

Fig. 3: EPM results from beam 2C - Red cells indicate a very high likelihood of corrosion

CHLORIDE INGRESS

Chloride content tests measure the ingress of chlorides into concrete. Chlorides from salt water diffuse into the concrete and when the concentration at the depth of reinforcement reaches the threshold value, corrosion can initiate. Chloride ingress was the principle cause of reinforcement corrosion on the Tiwai Point Bridge.

Chloride content testing involves drilling a hole into the concrete and taking samples of the drilling dust at depth intervals up to the depth of the reinforcement. The chloride content of these samples is then plotted against depth, and the chloride content at the depth of reinforcement is determined. When the concentration has not yet reached the corrosion threshold Fick's law of diffusion can be used to estimate the remaining time to initiation[6].

Extensive chloride sampling was conducted on beams from Tiwai Point, with three to six profiles collected from each of the nineteen test beams, and also from a number of other beams. These samples will be used to conduct a detailed study of the exposure conditions at the bridge site, with an emphasis on identifying the effects of the different microclimates that exist in different places on the structure.

An example of chloride ingress in the soffit of three beams is given in Fig. 4. A considerable difference in chloride content at the depth of reinforcement is observed between the good condition beam and the two corroding beams. Chloride ingress testing is a useful tool for assessing the likelihood that corrosion of steel is occurring in a given beam and for estimating the time to initiation, but is not useful for assessing the extent or location of corrosion in a beam that is known to be corroding. Full chloride ingress results are therefore excluded from this paper as they do not aid in the assessment of residual strength.

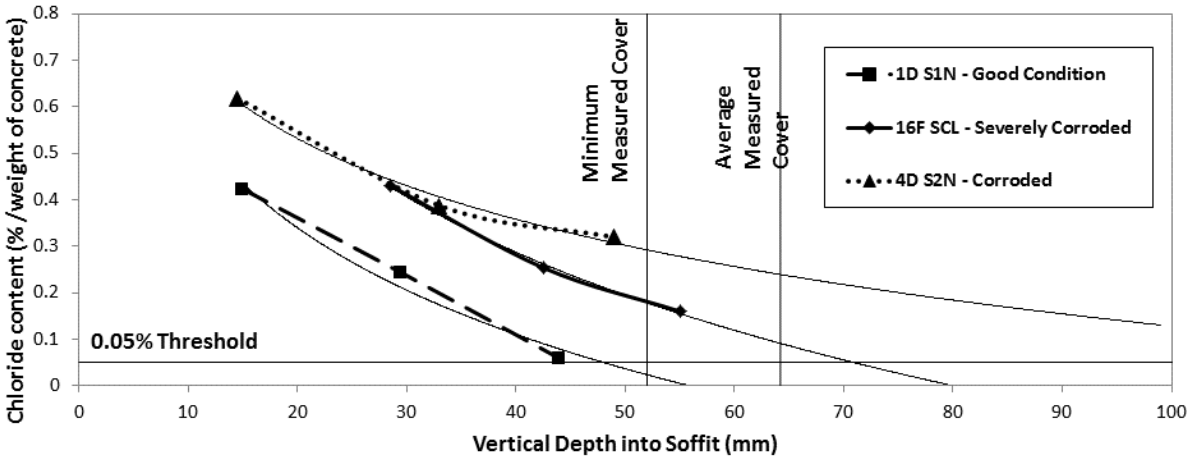

Fig. 4: Preliminary chloride ingress results

CARBONATION DEPTH

Carbonation is another cause of reinforcement corrosion and occurs when airborne carbon dioxide penetrates the concrete and causes the pH to decrease to the level where the alkalinity of the concrete no longer prevents reinforcement corrosion. Carbonation depth was measured by spraying a solution of phenolphthalein pH indicator onto a freshly cut concrete surface and measuring the depth of the colour change.

Carbonation measurements were performed on ten beams, and carbonation levels were found to be insignificant, with the average carbonation depth being less than 5 mm.

CONCRETE STRENGTH:

Schmidt Hammer readings were taken on all beams to assess concrete strength. These readings were calibrated against a total of six cores taken from four different beams. Typical average Schmidt hammer readings taken from the vertical face of the web were around 62.

This is near to the upper limit for the device and converts to a compressive strength of >58MPa. Calibration of the Schmidt hammer values against measured compressive strength results from collected core samples is yet to be performed. However, the compressive strength of core samples was measured at 66.5 MPa in a 2004 inspection[4] and 69 MPa and 56.7 MPa on cores taken during destructive testing.

CONDITION ASSESSMENT

Assessment of the condition of each beam requires an understanding of the process by which a single strand corrodes and the progression of the corrosion of strands within the beam. The beams with twelve pretensioned strands displayed a similar progression, which was different to that observed in beams with ten pretensioned strands.

CORROSION OF A SINGLE STRAND

There are a number of different mechanisms by which corrosion of a strand can occur. These are predominantly influenced by existing conditions in the surrounding concrete.

In the case of the Tiwai Point Bridge corrosion was initiated as a result of Chloride ingress resulting from sea water being deposited on the surface of the concrete. Chloride penetration into sound concrete is governed by Fick's laws of diffusion. When the concentration at the level of the strand reaches and exceeds the threshold value the likelihood of corrosion increases dramatically. Corrosion usually first initiates in a corner strand as these are exposed to chloride ingress from two sides. In sound concrete corrosion of a strand will manifest either uniformly over the surface of the steel, or as a concentrated pit. Both processes were observed on beams from the Tiwai Point Bridge and are shown in Fig. 5. As corrosion progresses the expansion of the corrosion product eventually causes a longitudinal crack to form at the level of the corroding steel. This crack causes a change in the surrounding concrete and thus in the corrosion process.

Fig. 5 Strands with uniform corrosion and individual wires with pitting damage

After longitudinal cracking of the concrete has occurred seawater and oxygen are more readily available to the corroding steel and the process accelerates. The cracking usually causes debonding of the lower part of the strand because the concrete is less stiff in the direction of the soffit. This forms a void below the strand where seawater collects, as shown in Fig. 6. This causes the strand to corrode uniformly upwards from the bottom to the top.

This type of corrosion was widespread in cracked regions of the corroded test beams, a typical example is shown in Fig. 6. Because strands are made up of six helical wires wrapped around a central wire all six of the helical wires rotate past the bottom of the strand in a length of less than 200 mm. Combined with the compromised bond in corroded and cracked regions it is not overly conservative to assume that 85% of the capacity of a strand is lost when corrosion has progressed one third of the height of the strand, this correlates to approximately 30% of the cross-sectional area. When corrosion has progressed two thirds of the height of the strand 100% of the capacity is lost.

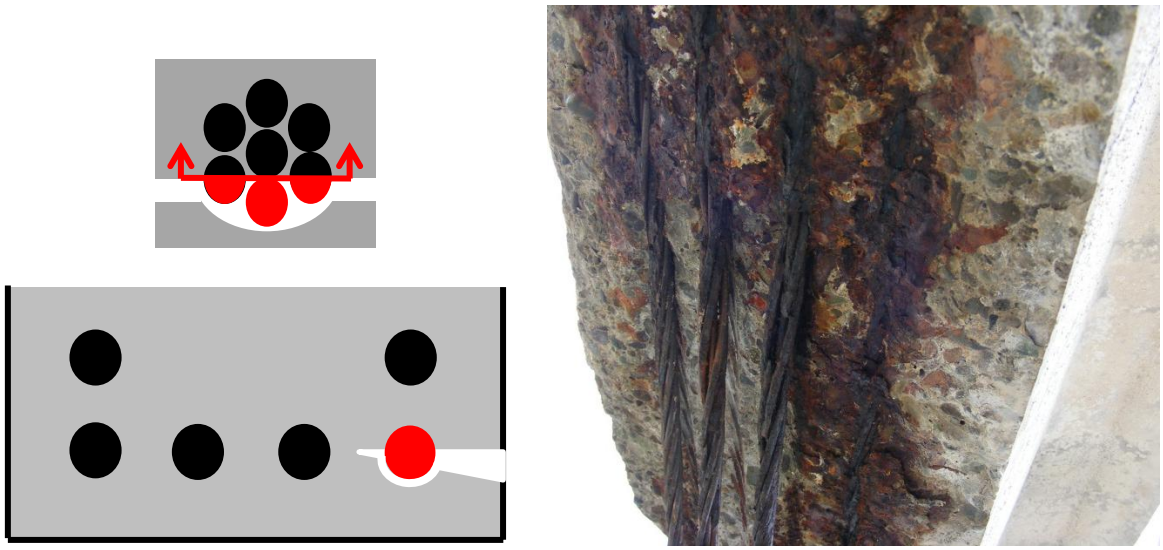

Fig. 6 Diagrams of crack and debonding, and evidence of upward strand corrosion

Because strands are made up of small wires they are faster to corrode when compared with conventional reinforcement bars. This is for two main reasons: firstly because the voids between the wires allow moisture and chlorides to build up and propagate easily and secondly because corrosion attacks the available steel surface and strands have a high surface area relative to their cross-sectional area.

The combination of processes described in this section result in the load carrying ability of a strand being rapidly reduced to effectively zero once a crack reaches it and debonding occurs. For this reason any strand that is determined to be intersected by a longitudinal crack should be assumed to be ineffective and neglected in the calculation of residual strength of the beam. This approach is only slightly conservative and more accurate than estimating the percentage of cross section lost and assuming that the remaining cross section is effective.

PROGRESSION OF CORROSION IN A BEAM

As corrosion in the corner strand progresses the crack widens and propagates further horizontally across the beam soffit.

In the beams with twelve pretensioned strands, four strands were present in the bottom layer. In these beams the crack intersected the adjacent strand in the bottom layer where the

debonding and upward corrosion process began again. Because both sides of each beam's web are subjected to very similar exposure environments and concrete conditions many of the beams had this process occurring concurrently on both sides of the web. This repeats until the crack reaches the opposite side of the web and the soffit concrete is completely delaminated. This is diagrammatically shown in Fig. 7 and an example is given of a beam after the delaminated soffit has fallen away during destructive testing, evidence of strand corrosion is visible on the spalled concrete section.

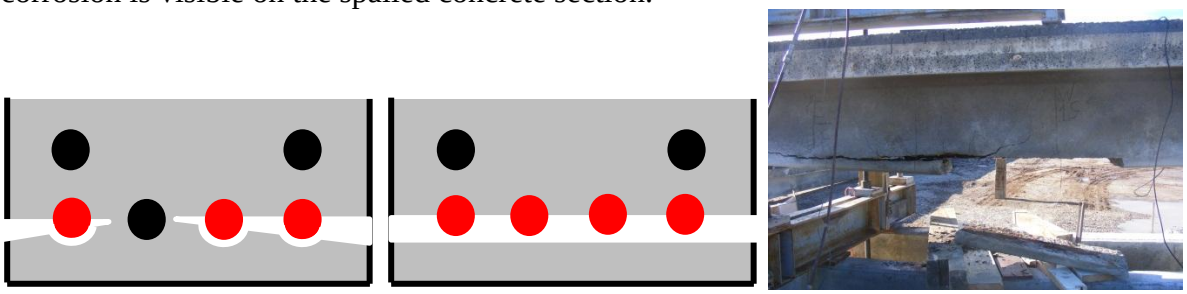

Fig. 7 Diagram of crack and debonding progression, and evidence of soffit delamination

In the beams with ten pretensioned strands there are only two strands on the edges of the bottom layer, so the crack did not intersect another strand but instead propagated downwards to the soffit and caused the corner concrete to spall. This exposed another surface for chloride ingress, which reduced the remaining time to initiation for the next strand.

CONDITION ASSESSMENT METHODOLOGY

The proposed methodology for assessing the condition of the corroded beams is based on assessing which stage of the cracking and debonding progression a given beam has reached. As explained in the previous sections once a crack has intersected a strand that strand is assumed to have lost its load carrying ability at the affected section.

The presence of a longitudinal crack on one side of a web implies that at least the nearest strand is corroding and has been intersected by the crack. The width of the crack and EPM results taken from areas surrounding the crack can indicate the severity of the corrosion and thus can be used to assess the likelihood that the crack has propagated and intersected the second and third strands.

By the time the crack has propagated to intersect the fourth strand only a small amount of sound concrete remains, so it is likely that delamination of the soffit would have occurred due to tensile forces caused by the opening of the crack. For this reason if a longitudinal crack is only visible on one side of the web it is fair to assume that at least one strand on the opposite side is intact.

The presence of longitudinal cracks on both sides of the web at a given section implies that at least the shallowest strand on both outside edges is corroding, and at worst that the soffit has delaminated exposing the entire layer of strands. The soffit should be checked for delamination by sounding with a hammer. If delamination has occurred all four strands are intersected by the crack and should be neglected. If delamination has not occurred it is likely

that at least one of the two central strands is not corroding, so one strand can be assumed to be effective. However, it is expected that a beam in this condition will quickly deteriorate to full delamination.

RESIDUAL STRENGTH ASSESSMENT

BACKGROUND

There has been a knowledge gap surrounding the assessment of the strength of concrete beams which have experienced pretensioned reinforcement corrosion. One contributing factor to this gap was a shortage of destructive test data from corroded pretensioned concrete bridge beams. This makes accurate assessment of the residual strength of beams difficult and often leads to bridges being replaced rather than rehabilitated. The strength assessment of corroded pretensioned beams is more complicated than for conventionally reinforced concrete beams because corrosion can cause relaxation of the steel and also causes the integrity of the bond between the steel and concrete to be compromised. Both of these effects reduce the amount of prestress that is transferred to the concrete and thereby weaken the structure considerably.

The bond between the steel and concrete is a difficult parameter to measure accurately even on a strand by strand basis, let alone for an entire beam or bridge. This makes assessment of the residual strength of a corroded pretensioned beam difficult and makes strengthening operations which would aim to restore lost prestressing force dangerous due to the risk of overstressing the concrete member.

OBJECTIVES AND OUTCOMES

The major objective of the residual strength assessment was to provide a correlation between non-destructive assessment methods and the measured strength of corroded pretensioned concrete bridge beams. This correlation was achieved by generating a large number of data points which relate the findings of a variety of non-destructive bridge assessment techniques to the measured flexural performance of full scale decommissioned concrete bridge beams.

The secondary objective was to generate information for a direct comparison tool which will be used by bridge consultants in the assessment of beams which have experienced pretensioned reinforcement corrosion. The information to be included in the tool is summarised in this paper.

SCOPE

The assessment consisted of destructive and non-destructive testing on nineteen beams which had experienced different degrees of corrosion to the pretensioned strand. Beams were selected for testing based on their prestressing design, location on the bridge and their degree of corrosion as assessed visually.

SUMMARY OF RESIDUAL STRENGTH ASSESSMENT RESULTS

Non Destructive Testing results are summarised in Table 1 along with data observed after breaking out concrete following destructive testing. EPM results provide a good correlation with corrosion damage and failure location; although in most cases the corrosion damage and failure location were also identified by the visual inspection. EPM did not detect any strand corrosion in areas that had not experienced cracking, which is consistent with the behaviour of the beams during destructive testing, as no strand breakages were detected by the Acoustic Emissions system.

Comparison of the crack patterns present on each beam with the number of corroded strands identified after breakout correlates well with the condition assessment methodology described in the previous section. All of the beams with cracking visible on both sides of the web had corrosion damage to between three and four of the strands in the bottom layer, while those with cracking on only one side (or on both sides but not at the same section) had damage to between one and three strands.

Table 1: Summary of NDT results compared to post-failure breakout

		Visual Inspection			EPM west		EPM east		Post-failure breakout			
	Beam Label	Longitudinal Cracking visible on side of web	max crack width west**	max crack width east**	Max in failure zone	average over 0.5m in failure zone	Max in failure zone	average over 0.5m in failure zone	Peak Load (kN)	no. of corroded strands*	failure location (from CL)	dominant failure mode
12 Strands, No Expansion Joint	14G	neither	0 mm	0 mm	282	254	272	246	346	0	4.5 m Nth	shear
	3C	neither	0 mm	0 mm	187	177	205	184	338	0	4.5 m Nth	shear
	18E	both	>2 mm	>2 mm	621	526	573	532	266	4	2 m Nth	flexural
	21F	both	2 mm	3 mm	577	526	494	449	260	3	1.5 m Sth	flexural
	3D	both	5 mm	4 mm	555	452	577	445	246	3.29	1.3 m Sth	flexural
	2C	both	3 mm	3 mm	572	442	509	430	233	4	1.4 m Sth	flexural
12 Strands, Expansion Joint	13F	neither	0 mm	0 mm	189	177	174	163	317	0	reached max stroke	
	1D	neither	0 mm	0 mm	171	124	190	178	310	0	2 m Nth	flexural
	4D	west	3 mm	0 mm	483	414	430	384	290	2.43	1.7 m Sth	flexural
	16G	both, not at same section	>2 mm	>2 mm	401	348	344	330	288	2.14	1.5 m Sth	flexural
	16F	both	>2mm	>2mm	476	418	460	389	215	4	1.5 m Sth	flexural
10Strand No Exp	3B	neither	0 mm	0 mm	182	172	210	197	311	0	1.5 m Sth	flexural
	2B	neither	0 mm	0 mm	201	175	188	177	300	0	2 m Sth	flexural
	21I	west	5 mm	0 mm	461	415	340	280	270	1	1.4 m Sth	flexural

*the whole number represents completely corroded strands. The number after the decimal point represents partial damage to one strand, expressed as the number of corroded wires divided by 7. No beam had partial damage to more than one strand

**Beams that underwent testing early in the program did not have accurate crack width measurements

DESTRUCTIVE TESTING

Destructive testing was undertaken on beams with three of the four prestressing arrangements as described in the design and construction section, and the results from each of the groups are analysed independently. Selection of beams for each group was performed by grading based on the amount of longitudinal cracking evident on the sides of the web. The condition of each test beam was confirmed after testing by breaking out areas of concrete to expose reinforcement. A summary of the nineteen tests is given below in Table 2.

Table 2: Summary of destructive tests

	Good Condition	*Corroded Pretension*	*Total Tests*
12 pretensioned, without expansion joint	2	4	6
12 pretensioned, with expansion joint	2	3	5
10 pretensioned, without expansion joint	2	1	3
No expansion joint and cut pretensioning	1	0	1
Expansion joint and cut pretensioning	1	0	1
10 pretensioned and cut posttensioning	1	0	1
Data requires further post processing	1	1	2

TEST SETUP

The beams were tested in a simply supported state using a four point loading system. Due to the remote location of the bridge, the large size of the test specimens and the extensive testing regime, the cost to transport and test the beams at the University of Auckland was prohibitive. The testing was therefore carried out on site using a purpose built self-reacting load frame constructed from three of the decommissioned bridge beams, a steel yoke and tension ties. The rig was designed to cause flexural failure in the specimens, and to approximate an axle loading condition. The test setup is shown in Fig. 8.

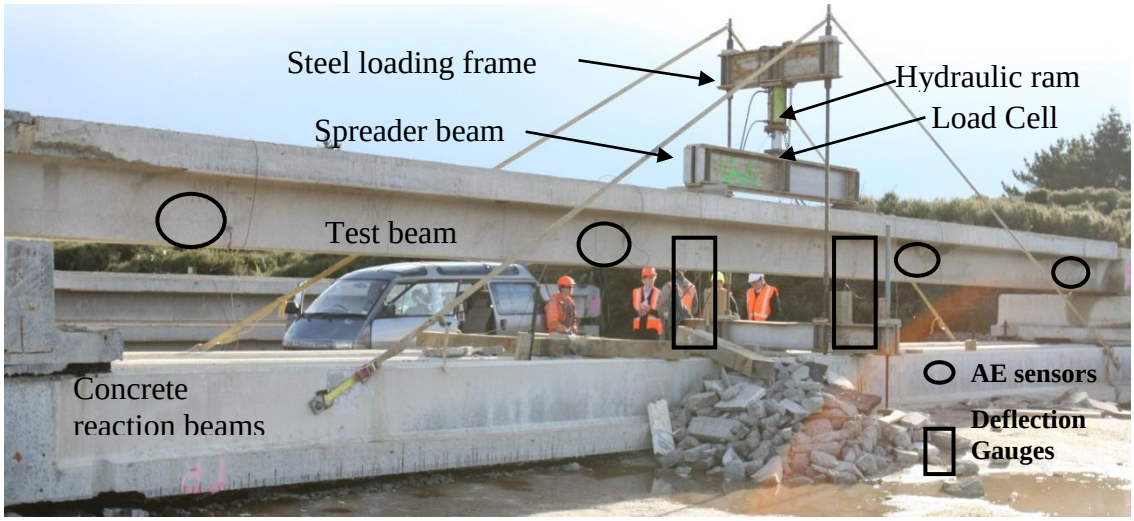

Fig. 8: Picture of self-reacting load frame for destructive testing

The destructive testing phase commenced after the NDT phase and was concurrent with the deconstruction of the second half of the bridge. As the deconstruction of the bridge continued the final test beams were selected and the remaining NDT tests carried out on those beams.

Load was applied to the asphalt surfacing on the test beams through two 100 mm wide line loads across the width of the flange. The line loads were located 1.5 m either side of mid span and were applied through a simply supported spreader beam by a single 1000 kN hydraulic ram at mid-span. Load was measured using a load cell on the ram, and deflections were measured relative to the ground below each of the line loads. Deflection of the end supports was also measured relative to the ground and the beam deflections were adjusted to account for this support deflection. Load readings do not take into account the self-weight of the beams.

Acoustic Emissions (AE) monitoring equipment was used to detect damage during the destructive testing. The primary reason for the AE system was to identify and locate prestressing strand breakage and compare that to corrosion sites identified with non-destructive testing. A secondary aim of the AE monitoring was to identify and distinguish between different types of structural damage as they occurred during the tests. The AE data was time stamped and recorded concurrently with load and deflection data. Failure of reinforcement was only observed in strands which had experienced severe corrosion. Failed strands were exclusively in the bottom or second layer of pretensioned reinforcement with the majority being in the bottom layer. Failed strands were only detected in areas with external evidence of corrosion.

TEST RIG CONSTRUCTION

The tests were performed in a number of stages scheduled to fit into the deconstruction programme. The first stage involved the construction of the components required for the destructive loading frame. This process involved the manufacture of four heavy steel beams, which along with several high tensile rods formed the central part of the frame, and the preparation of four of the bridge beams to form the longitudinal reaction beams and end supports. The bridge beams selected to be used as reaction beams were rolled upside down and positioned, then the lower part of the central tower was assembled. The end support beam sections were placed and bolted down, and the first test unit was positioned on the rig. The spreader beam was placed on top of the test unit. The top part of the tower was assembled on the ground and then lifted on to the test rig and attached using couplers on the vertical high tensile rods and ratchet strops for stability. Fig. 9 shows the completed test rig.

Fig. 9: Test rig and deflected beam 4C

LOADING PROCEDURE

The loading procedure for the beams was complicated by the stroke of the hydraulic ram. The stroke capacity of the jack was approximately 250 mm and the beams failed at deflections of around 400 mm. For this reason the beams were loaded to full stroke and then propped using the timber struts shown in Fig. 9. The hydraulic ram was then retracted and a packer inserted, allowing the load to be reapplied through the packer once the timber struts were removed. This process was repeated until sufficient deflection capacity was made available. This resulted in the load reading dropping to zero as the load was transferred to the timber struts while the beam remained deflected. This portion of the data has been removed from the load deflection graphs to reduce clutter, but is evidenced by the two small drops in load at approximately 225 mm and 250 mm deflection.

FAILURE MODES

The load-deflection response of all three beam types was similar. Good condition beams deflected evenly and displayed regularly spaced vertical flexural cracks over the middle third of the span. Some beams in good condition also displayed a pure web shear crack approximately 2 m from the support point, just outside the haunch of the beam. The shear cracks coincided with the end of the debonding of the bottom 4 to 6 pretensioned strands. In all but two cases the beams in good condition failed at one of the loading points with a flexural shear crack extending from outside the loading point and penetrating into the flange, followed by crushing of the concrete in the compression zone. In the exceptional cases the beam displayed a shear failure beginning 2 m from the end of the beam and spreading to the nearest load point. Examples of the typical failure mode for good condition beams are given in

Fig. 10. The bottom image shows the failure crack; concrete crushing is evident under the loading point and the longitudinal reinforcement is intact and visible where the cracked concrete in the tension zone has fallen away during failure of the beam. The AE system detected no strand breakage during the good condition tests and this was confirmed by breakout and inspection around the failure plane.

Fig. 10: Typical good condition beam failures

The deflection of beams with corrosion damage was typically concentrated around the damaged area. Flexural cracking would extend up and outwards from the original corrosion crack and the soffit would spall off at a low deflection. The Acoustic Emission system did not detect any strand failures outside of the corroded area that ultimately failed. Typical cracking patterns for corroded beams are shown in the top two images of Fig. 11. Usually failure would occur at a loading point, with the failure crack extending from the corroded area to meet the loading point, as shown in the two bottom images in Fig. 11. If the corroded area was too far away from the loading point, the strands would fail at the corroded section

and then pull through to a separate failure crack closer to the loading point; this can be seen in the bottom right image.

Fig. 11 Typical corroded beam cracking and failure

CONTROL TESTS AND COMPARISON OF PRESTRESSING ARRANGEMENTS

Destructive testing was performed on three of the four different prestressing arrangements existing on the bridge. Fig. 12 below shows a comparison between beams in good condition containing each of the three different prestressing arrangements that were subjected to testing. These beams displayed similar ductility characteristics and a 12% difference in ultimate load between the strongest and weakest of those tested, with the fourth prestressing type expected to be the weakest.

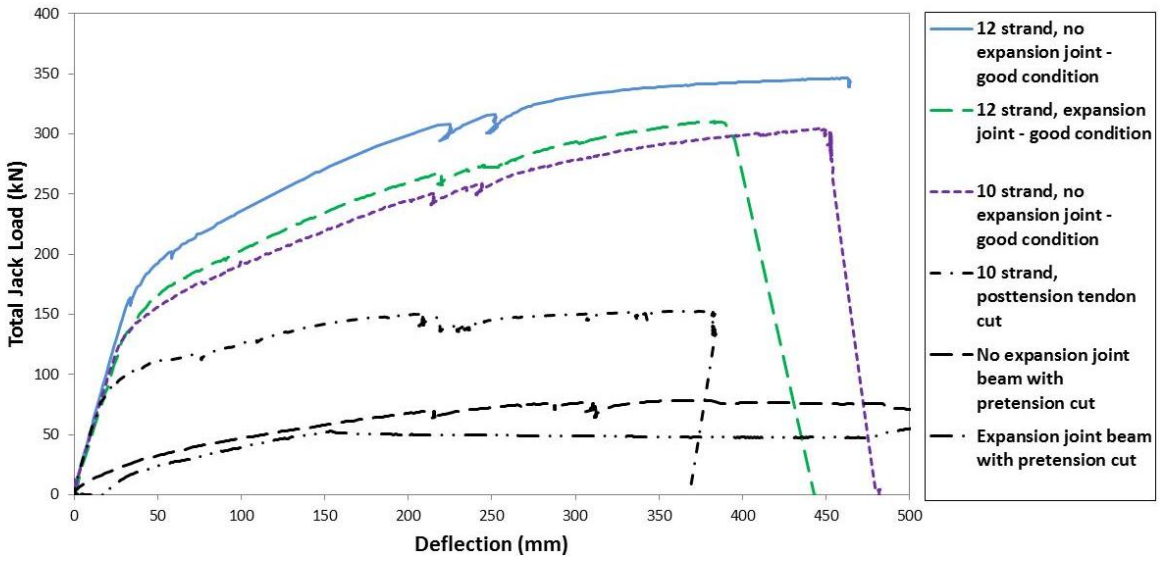

Fig. 12: Control test results and prestressing arrangement comparison

Three control tests were also carried out to isolate the two differing post tensioned tendon drapes and the pretensioned reinforcement. The control tests were performed by cutting all of either the pretensioned or the posttensioned reinforcement, to isolate the other. The reinforcement was cut as close as possible to the failure locations displayed by full strength beams. Load deflection plots from the control tests are given in Fig. 12, showing that the strength contribution from the pretensioned strand is considerably greater than that from the posttensioned tendon, and that the two different drapes resulted in a small difference in strength.

TWELVE PRETENSIONED STRANDS WITHOUT EXPANSION JOINT

Six tests were performed on beams with twelve pretensioned strands and no expansion joint, two were on good condition beams and four tests were on beams displaying corrosion damage to the pretensioned reinforcement. The six load-deflection plots are displayed in Fig. 13. The average ultimate strength of the beams in good condition was 342.5 kN, whereas the weakest of the corroded beams supported only 68% of this load. Post-test inspection revealed that the weakest beam had corrosion damage to all four strands in the bottom layer of pretensioned reinforcement, evidenced by a 1200 mm crack 1.5 m from mid-span that was visible on both sides of the web.

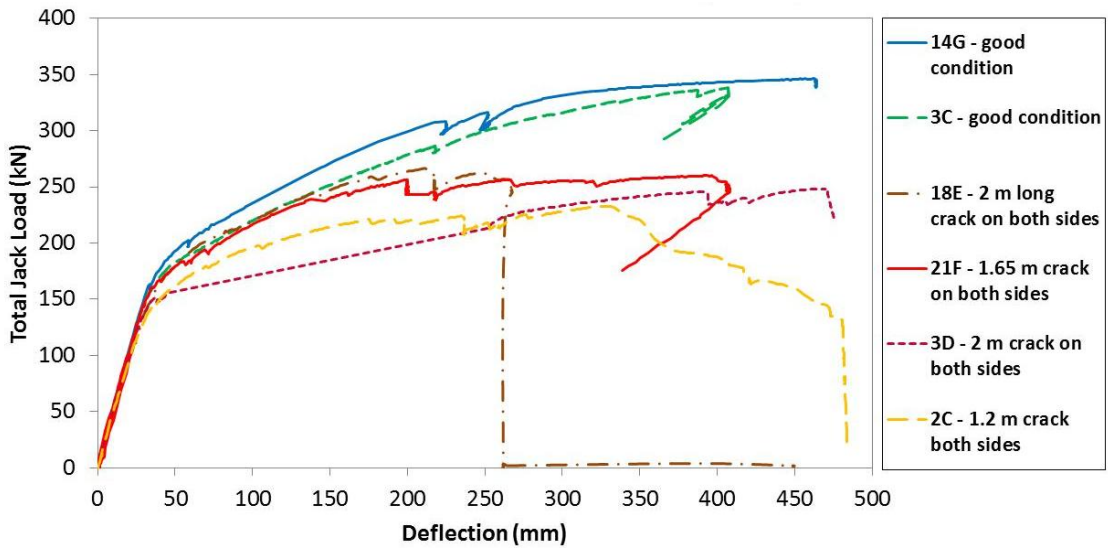

Fig. 13: Load vs. deflection: 12 pretensioned strands, no expansion joint

TWELVE PRETENSIONED STRANDS WITH EXPANSION JOINT

Five tests were carried out on beams with twelve pretensioned strands and an expansion joint. Two tests were on beams in good condition and four tests were on beams displaying corrosion damage to the pretensioned reinforcement. Load-deflection plots are displayed in Fig. 14. The average ultimate strength of the beams in good condition was 313.5 kN, whereas the weakest of the corroded beams supported only 69% of its good condition counterpart. Post-test inspection revealed that the weakest beam had corrosion damage to all four strands in the bottom layer of pretensioned reinforcement, which was evidenced by cracking and spalling of the lower part of the web and soffit over a length of 2.2 m extending outwards from near to mid-span.

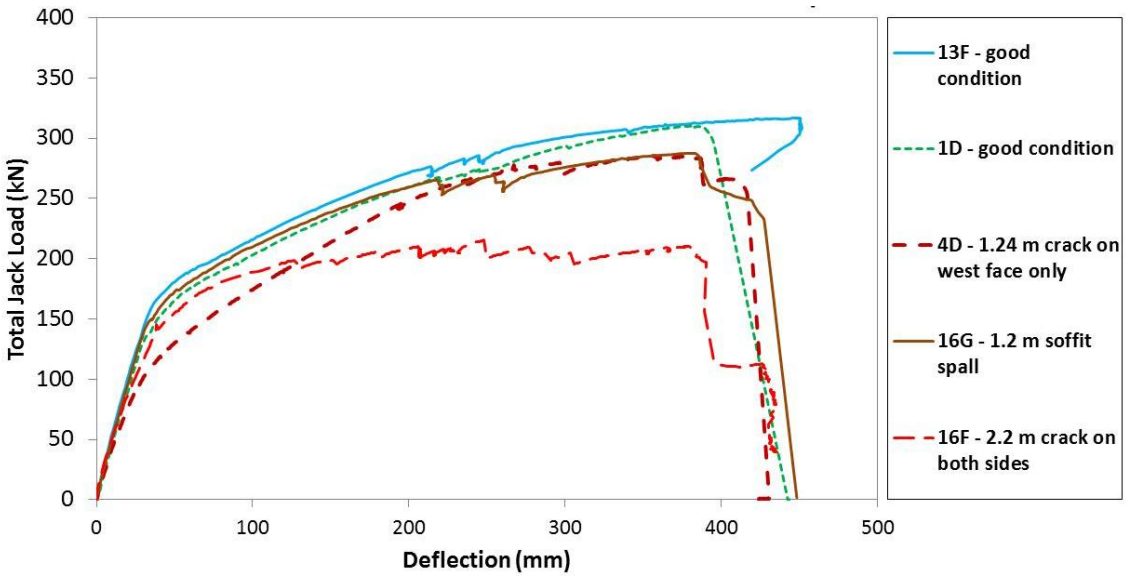

Fig. 14: Load vs. deflection: 12 pretensioned strands with expansion joint

TEN PRETENSIONED STRANDS, WITHOUT EXPANSION JOINT

Three tests were carried out on beams with ten pretensioned strands and no expansion joint. Two tests were on beams in good condition and one test was on a beam displaying corrosion damage to the pretensioned reinforcement. Load-deflection plots are displayed in Fig. 15. The average ultimate strength of the beams in good condition was 301 kN, whereas the corroded beam sustained 90% of its good condition counterpart. This weaker beam had corrosion damage to one of the two pretensioned strands in the bottom layer of reinforcement, which was evidenced by an 800 mm long crack visible on only one side of the web.

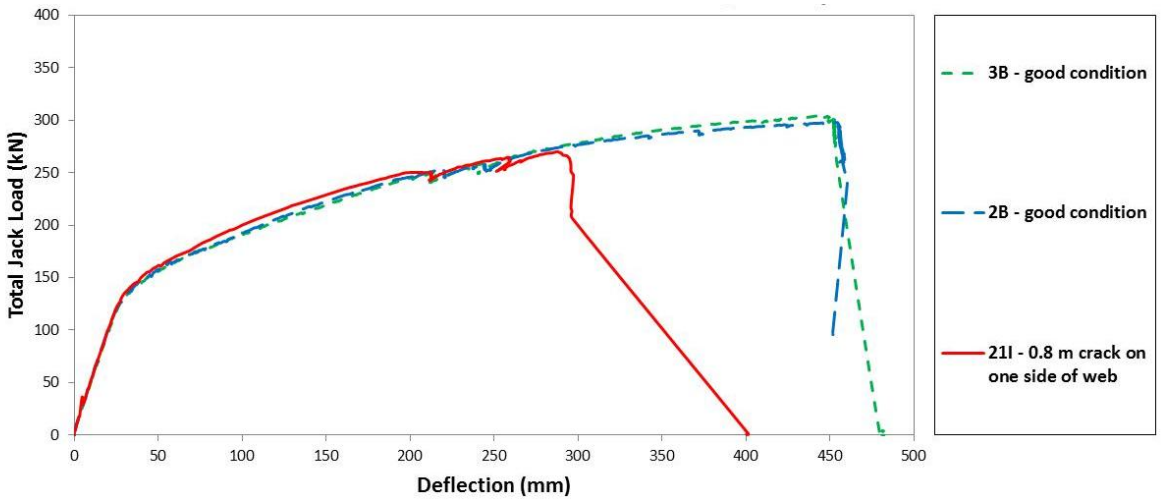

Fig. 15: Load vs. deflection: 10 pretensioned strands, no expansion joint

CONCLUSION

Nineteen destructive tests were carried out on beams with three different designs from the Tiwai Point Bridge. Good condition beams of similar design displayed very similar load deflection behaviour. All beams which displayed corrosion of the pretensioned reinforcement had reduced capacity; strength loss was approximately proportional to the number of strands affected by corrosion. The worst condition beams had damage to all four strands in the bottom layer and achieved strengths of 68% and 69% of their good condition counterparts.

The progression of corrosion damage observed in the beams was described and a model was presented for assessment of the beams using non-destructive means. The recommendations of this model were compared with actual damage as assessed by breakouts after destructive testing. The non-destructive procedure provided an effective means of estimating the number of corroded strands that should be disregarded in calculation of the residual strength of a damaged beam.

REFERENCES

1. Thomas, C., and Coles, G., "Tiwai Bridge Options Study Summary Report." MWH, 2006, Invercargill.
2. Thomas, C., and Coles, G., "Tiwai Bridge Posting Review." MWH, 2006, Invercargill.
3. Bruce, S. M., McCarten, P. S., Freitag, S. A., and Hasson, L. M., "Deterioration of Prestressed Concrete Bridge Beams." *Land Transport New Zealand Research Report 337*, Land Transport New Zealand, 2008, Wellington, 72.
4. Thomas, C., and Kensington, D., "Tiwai Bridge Evaluation and Repair Design."*RICC01*, MWH, 2004, Invercargill.
5. Thomas, C., and Coles, G., "Tiwai Bridge Visual Inspection." MWH, 2008, Invercargill.
6. Broomfield, J. P., "Corrosion of steel in concrete: understanding, investigation and repair", Taylor & Francis, 2007, 1997, London; New York.